Critical dynamics of phase transition driven by dichotomous Markov noise

Katsuya Ouchi*

Kobe Design University, 8-1-1 Gakuennishi-machi, Kobe 651-2196, Japan

Takehiko Horita†

Department of Mathematical Informatics, The University of Tokyo, 7-3-1 Hongo, Bunkyo-ku, Tokyo 113-8656, Japan

Hirokazu Fujisaka‡

Department of Applied Analysis and Complex Dynamical Systems, Graduate School of Informatics, Kyoto University, Kyoto 606-8501, Japan

An Ising spin system under the critical temperature driven by a dichotomous Markov noise (magnetic field) with a finite correlation time is studied both numerically and theoretically. The order parameter exhibits a transition between two kinds of qualitatively different dynamics, *symmetry-restoring* and *symmetry-breaking motions*, as the noise intensity is changed. There exist regions called channels where the order parameter stays for a long time slightly above its critical noise intensity. Developing a phenomenological analysis of the dynamics, we investigate the distribution of the passage time through the channels and the power spectrum of the order parameter evolution. The results based on the phenomenological analysis turn out to be in quite good agreement with those of the numerical simulation.

I. INTRODUCTION

Over the last decade, the dynamics of ferromagnetic systems below their critical temperatures in a periodically oscillating magnetic field have been studied both theoretically [1–9] and experimentally [10]. The systems exhibit two qualitatively different behaviors referred to as *symmetry-restoring oscillation* (SRO) and *symmetry-breaking oscillation* (SBO), depending on the frequency Ω and the amplitude h of the applied magnetic field. It has been established that there exists a sharp transition line between SRO and SBO on the (Ω, h) plane, which is called the *dynamical phase transition* (DPT). The DPT was first observed numerically in the deterministic mean-field system for a ferromagnet in a periodically oscillating field [1], and has subsequently been studied in numerous Monte Carlo simulations of the kinetic Ising system below critical temperature [2–6]. It has also been observed experimentally in an ultrathin Co film on Cu(100) [10].

Recently, we investigated the DPT by introducing the model equation $\dot{s}(t) = (T_c − T)s − s^3 + h \cos \Omega t$ [7]. This equation is a simplified model for the Ising spin system at temperature T below its critical value T_c in an external periodic magnetic field. By appropriately scaling the magnetization s, time t, and the applied field, this equation is written as

$$\dot{s}(t) = s − s^3 + h \cos \Omega t. \tag{1}$$

The SBO and SRO are observed in Eq. (1) and the transition line between them on the (Ω, h) plane is determined analytically [7,8].

It is quite interesting to ask whether DPT is observed under another kind of applied field, especially random field with bounded amplitude. The fundamental aim of the present paper is to study the dynamics of $s(t)$ with a dichotomous Markov noise (DMN) $F(t)$ instead of periodically oscillating external field $h \cos \Omega t$ (see, e.g., Ref. [11]).

The equation of motion

$$\dot{s} = f(s) + F(t) \tag{2}$$

with a nonlinear function $f(s)$ and the DMN $F(t)$ has been extensively studied by many authors [12–15]. It is well known that the master equation for the system can be derived, and then transition phenomena of stationary probability densities concerning the intensity of $F(t)$, for example, are studied, which are referred to as the noise-induced phase transition [12,16]. The asymptotic drift velocity $\langle \dot{s} \rangle$ in the case of $f(s)$ being periodic functions are also discussed as a specific dynamic property [13]. Furthermore, the mean first-passage time (MFPT) and transition rates are investigated as another important dynamic property when $f(s)$ is the force associated with the bistable potential given by Eq. (2) [14,15]. For a review of works on DMN system, see Bena [17].

The fundamental aim of the present paper is to propose a phenomenological approach to the critical dynamics near the transition point between the symmetry-restoring motion (SRM) and the symmetry-breaking motion (SBM) observed in Eq. (2) with $f(s) = s − s^3$ (Sec. II) and to investigate the distribution of passage times through channels, switching

*Electronic address: ouchi@kobe-du.ac.jp

†Present address: Department of Mathematical Sciences, Osaka Prefecture University, 1-1 Gakuencho, Sakai, Osaka 599-8531, Japan; Electronic address: horita@ms.osakafu-u.ac.jp
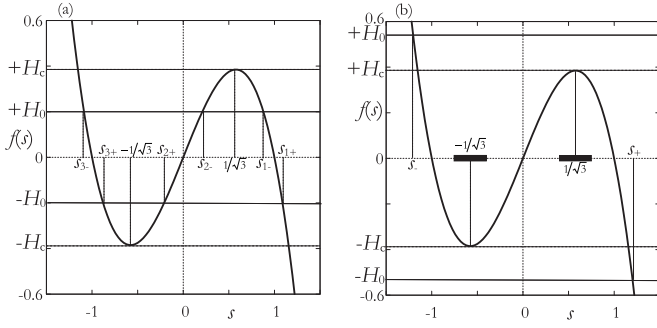
‡Electronic address: fujisaka@i.kyoto-u.ac.jp

FIG. 1. The function $f(s) = s - s^3$ is shown by solid lines. (a) Real roots $s_{j\pm}$, $(j=1,2,3)$ for $H_0 < H_c$ and (b) real roots $s_\pm$ for $H_0 > H_c$ of the algebraic equation $s - s^3 \pm H_0 = 0$. The definition of H_c is graphically represented. Two bold lines drawn in (b) indicate the channel regions defined in Sec. III.

times between two different motions, and the power spectrum of the order parameter evolution. The present paper is constructed as follows. In Sec. II, we discuss the dynamics of symmetry-breaking motion and symmetry-restoring motion of the model equation (2). In Sec. III, the jumping process of the magnetization through channels, which are defined in the text, is investigated and the MFPT is obtained. In Sec. IV, a phenomenological approach simplifying the dynamics of passing through a channel in the SRM phase is introduced and three statistical characteristics are analytically developed. The results are compared with numerical simulations. Concluding remarks are given in Sec. V.

II. MODEL EQUATION AND SYMMETRY-BREAKING TRANSITION

A. Model equation and noise-induced phase transition

We consider the equation of motion driven by the external field $F(t)$,

$$\frac{ds(t)}{dt} = f(s) + F(t) \quad [f(s) = s - s^3], \qquad (3)$$

where $F(t)$ is a symmetric DMN with taking the values $\pm H_0$. Here the probability $p(\tau)$ that $F(t)$ continues to take the iden-

tical value $+H_0$ or $-H_0$ longer than time τ is given by

$$p(\tau) = e^{-\tau/\tau_f}. \qquad (4)$$

This implies that the correlation time of $F(t)$ is equal to $\tau_f/2$. Throughout this paper, numerical integrations of Eq. (3) are carried out by using the Euler difference scheme with the time increment $\Delta t = 1/100$.

Without DMN, $s(t)$ eventually approaches either of the stationary fixed points ± 1, one of which is achieved according to the initial condition $s(0)$ as shown in Fig. 1. In the presence of DMN, if $H_0 < H_c$, H_c being defined by

$$H_c \equiv 2(1/3)^{3/2} = 0.3849 \cdots , \qquad (5)$$

then $f(s) + H_0 = 0 [f(s) - H_0 = 0]$ has three real roots $s_{j+}(s_{j-})$ $(j=1, 2, \text{and } 3)$. Each value of $s_{j\pm}$ is graphically shown in Fig. 1(a). On the other hand, if $H_0 > H_c$, then $f(s) + H_0 = 0$ $[f(s) - H_0 = 0]$ has only one real root s_+ (s_-) given by

$$s_\pm = \left[\tfrac{1}{2}(\pm H_0 + \sqrt{H_0^2 - H_c^2}) \right]^{1/3} + \left[\tfrac{1}{2}(\pm H_0 - \sqrt{H_0^2 - H_c^2}) \right]^{1/3}, \qquad (6)$$

which are indicated in Fig. 1(b).

Next let us consider the dynamics described by Eq. (3) for $H_0 < H_c$ and for $H_0 > H_c$, and discuss similarity and difference between the dynamics in the periodically oscillating field case and those in the present DMN case. A part of our results belongs to the context of the noise-induced phase transition and MFPT in Refs. [12–16]. In the case of $H_0 < H_c$, three motions numerically integrated are shown in Figs. 2(a) and 2(b). Two motions confined in the ranges $s_{1-} < s(t) < s_{1+}$ and $s_{3-} < s(t) < s_{3+}$ are both stable. The long time average $\langle s(t) \rangle$ of each motion does not vanish, and the motion is called SBM in relation to DPT in the oscillating external field case. On the other hand, the motion $s_u(t)$ confined in the range $s_{2+} < s_u(t) < s_{2-}$ is unstable. The long time average of $s_u(t)$ vanishes, and in this sense the motion is called SRM. It should be noted that this unstable SRM is located between two stable SBM, which has a similar characteristic to SBO of DPT [7].

The motion of $s(t)$ for $H_0 > H_c$ is shown in Figs. 2(c) and 2(d). One observes that there exists a stable SRM confined in
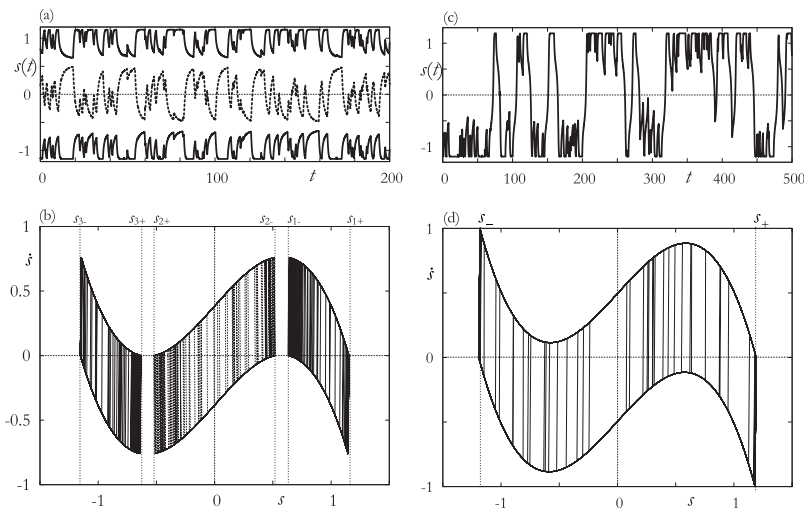

FIG. 2. (a) and (b) show the motions obtained by numerically integrating Eq. (3) for $H_0 = 0.38$ $(<H_c)$ and $\tau_f = 5$, where two SBM's (solid line) and an unstable SRM (dashed line) are drawn. The unstable SRM is evaluated by replacing $t \rightarrow -t$. On the other hand, (c) and (d) show the motions for $H_0 = 0.5$ $(>H_c)$ and $\tau_f = 10$.
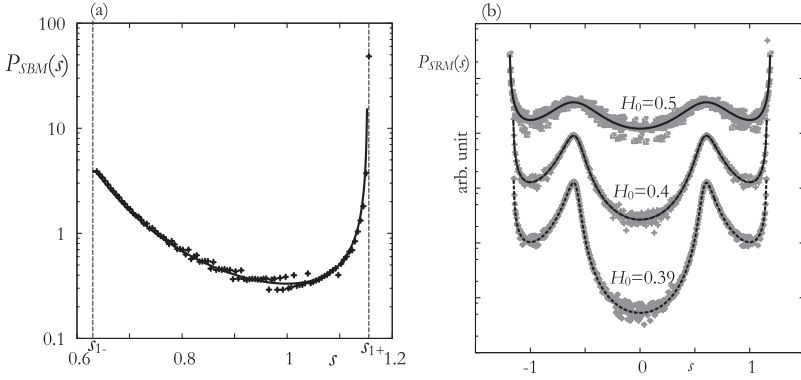
FIG. 3. Stationary distribution functions obtained both analytically (solid line) and numerically (symbols) for (a) $H_0=0.3$ and $\tau_f=5$, and for (b) $H_0=0.39$, 0.4, and 0.5 by keeping $\tau_f=10$. (a) and (b) correspond, respectively, to SBM and SRM. The distribution only in the range $s_{1-}<s(t)<s_{1+}$ is drawn in (a). The analytical result is in good agreement with that of the numerical simulation.

the range $s_-<s(t)<s_+$. For SRM, the time average of $s(t)$ vanishes, i.e., $\langle s(t)\rangle=0$. The comparison between Figs. 2(b) and 2(d) suggests that the SRM for $H_0>H_c$ is generated via the "attractor merging crisis" [18] of the two SBM's and one unstable SRM, i.e., the two SBM's and one unstable SRM disappear and then one stable SRM takes place at $H_0=H_c$. This situation is similar to that in the DPT case. However, in contrast to the DPT case, as will be shown in Sec. II B, the transition line on the (τ_f^{-1},H_0) plane is independent of the correlation time τ_f of $F(t)$ and the average $\langle s(t)\rangle$ depends discontinuously on H_0.

B. Stationary distribution functions and phase diagram

In this section, we discuss the stationary distribution functions for SBM and SRM. To this aim, we first consider a slightly general nonlinear Langevin equation of motion driven by DMN,

$$\dot{x}(t) = f(x) + g(x)F(t), \tag{7}$$

where $f(x)$ and $g(x)$ are generally nonlinear functions of x and $F(t)$ is DMN [19]. The temporal evolution of the distribution function $P(x,F,t)$ that $x(t)$ and $F(t)$, respectively, take the values x and F ($=\pm H_0$) is determined by [12,16]

$$\frac{\partial}{\partial t}P(x,t) = -\frac{\partial}{\partial x}[f(x)P(x,t) + H_0g(x)q(x,t)],$$

$$\frac{\partial}{\partial t}q(x,t) = -\frac{2}{\tau_f}q(x,t) - \frac{\partial}{\partial x}[f(x)q(x,t) + H_0g(x)P(x,t)], \tag{8}$$

where we set $P(x,t) \equiv P(x,+H_0,t) + P(x,-H_0,t)$ and $q(x,t) \equiv P(x,+H_0,t) - P(x,-H_0,t)$. The stationary distribution $P^{st}(x) \equiv P(x,\infty)$ is solved to yield

$$P^{st}(x) = N\frac{g(x)}{H_0^2g(x)^2 - f(x)^2}\exp\left[-\frac{1}{\tau_f}\int^x dx'\right.$$
$$\left.\times\left(\frac{1}{f(x')-H_0g(x')} + \frac{1}{f(x')+H_0g(x')}\right)\right], \tag{9}$$

provided that each of the equations

$$\dot{x} = f(x) + H_0g(x), \quad \dot{x} = f(x) - H_0g(x) \tag{10}$$

has at least one stable fixed point, where N is the normalization constant.

By substituting $f(x)=x-x^3$ and $g(x)=1$ [Eq. (3)], into Eq. (9), the stationary distribution function $P^{st}_{SBM}(s)$ for SBM ($H_0<H_c$) for $s_{3-}<s<s_{3+}$ or $s_{1-}<s<s_{1+}$ is written as

$$P^{st}_{SBM}(s) \propto |s^2-s^2_{1+}|^{-\beta_{1+}}|s^2-s^2_{1-}|^{-\beta_{1-}}|s^2-s^2_{2+}|^{-\beta_{2+}}, \tag{11}$$

$$\beta_{j\pm} = 1 - \tau_f^{-1}|(s_{j\pm}-s_{k\pm})(s_{j\pm}-s_{l\pm})|, \tag{12}$$

where $(j,k,l)=(1,2,3)$, $(2,3,1)$, and $(3,1,2)$. On the other hand, the stationary distribution function $P^{st}_{SRM}(s)$ for the SRM ($H_0>H_c$) for $s_-<s<s_+$ is obtained as

$$P^{st}_{SRM}(s) \propto |s^2-s^2_+|^{[\tau_f^{-1}/(3s^2_+-1)]-1}$$
$$\times[(s^2+s^2_+-1)^2-s^2_+s^2]^{-[\tau_f^{-1}/(3s^2_+-1)]-1}$$
$$\times\exp\left\{\frac{\tau_f^{-1}s_+}{(s^2_+-1/3)\sqrt{3s^2_+-4}}\left[\arctan\left(\frac{2s-s_+}{\sqrt{3s^2_+-4}}\right)\right.\right.$$
$$\left.\left.-\arctan\left(\frac{2s+s_+}{\sqrt{3s^2_+-4}}\right)\right]\right\}. \tag{13}$$

The analytic solutions (11) and (13) are numerically confirmed in Fig. 3.

As H_0 is increased, the form of the stationary distribution function changes drastically from the forms in Eq. (11) to Eq. (13) at $H_0=H_c$. This phenomenon which is induced by the disappearance of two pairs of stable and unstable fixed points [13] is an example of the noise-induced phase transitions [16]. It turns out that the transition line between SRM and SBM on the (τ_f^{-1},H_0) plane is given by $H_0=H_c$. The phase diagram is given in Fig. 4. Furthermore, the long time average of $s(t)$, $\langle s(t)\rangle$, depends discontinuously on H_0 at $H_0=H_c$ as shown in Fig. 5. These behaviors are quite different from those of the DPT case driven by periodically oscillating field, $F(t)=h\cos(\Omega t)$ [3,7]. The transition point h_c for a fixed Ω between SRO and SBO depends on the frequency Ω, and $\langle s(t)\rangle$ is a continuous function of h.

III. MFPT THROUGH THE CHANNELS

We hereafter discuss the dynamics for H_0 slightly above H_c. Let us first consider the behavior obeying the equations
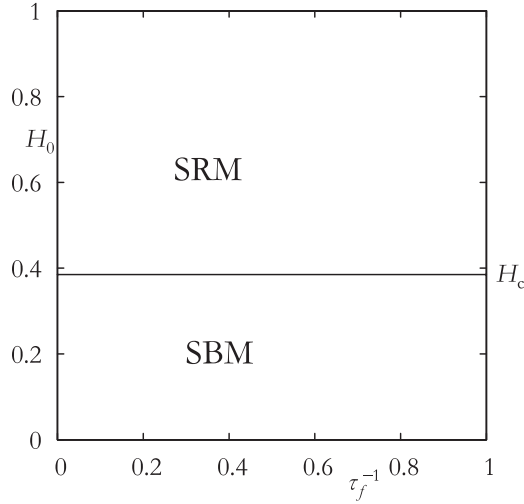
FIG. 4. Phase diagram on the (τ_f^{-1}, H_0) plane. Transition line is independent of τ_f^{-1} and is given by $H_0 = H_c$.

$$\dot{s} = s - s^3 + \epsilon H_0 \quad (\epsilon = + \text{ or } -) \tag{14}$$

for $H_0 > H_c$, i.e., $F(t)$ is fixed to be either $+H_0$ or $-H_0$. Equation (14) for $H_0 > H_c$ is integrated to yield

$$t = -\frac{1}{2(3s_\epsilon^2 - 1)} \ln \frac{(s - s_\epsilon)^2}{s^2 + s_\epsilon s + s_\epsilon^2 - 1}$$

$$\times \frac{s_0^2 + s_\epsilon s_0 + s_\epsilon^2 - 1}{(s_0 - s_\epsilon)^2} + \frac{6s_\epsilon}{2(3s_\epsilon^2 - 1)\sqrt{3s_\epsilon^2 - 4}}$$

$$\times \left[\arctan\left(\frac{2s + s_\epsilon}{\sqrt{3s_\epsilon^2 - 4}} \right) - \arctan\left(\frac{2s_0 + s_\epsilon}{\sqrt{3s_\epsilon^2 - 4}} \right) \right], \tag{15}$$

where $s_0 = s(0)$ and s_ϵ has been defined in Eq. (6). Figure 6 displays three orbits given by Eq. (15) with $s_0 = s_-$ and $\epsilon = +$, which shows that $s(t)$ approaches s_+ in the limit $t \to \infty$. One observes that $s(t)$ stays for a long time in the vicinity of s
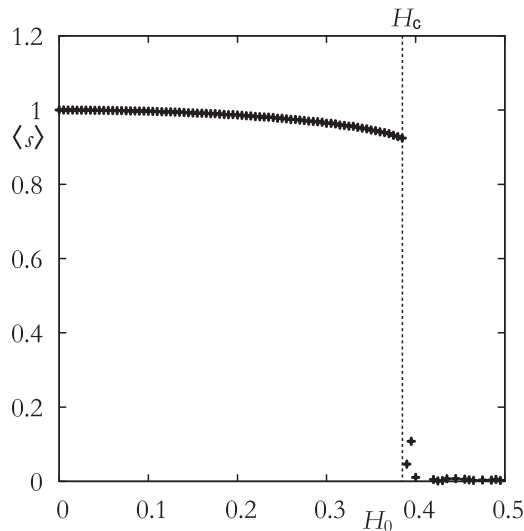

FIG. 5. $\langle s \rangle$ vs H_0 for $\tau_f = 5$. One finds that $\langle s \rangle$ is discontinuous at $H_0 = H_c$.
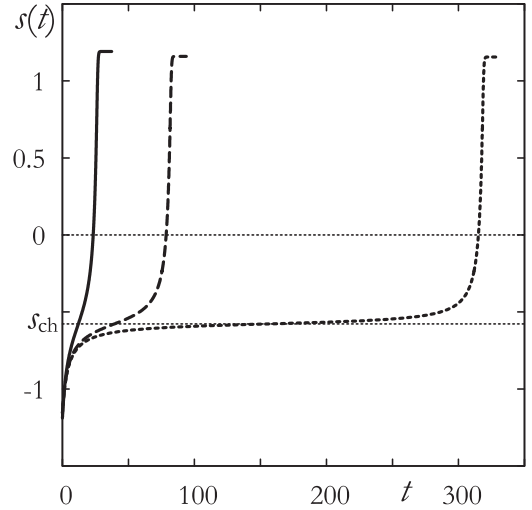

FIG. 6. Three orbits of the equation of motion (14) with $\epsilon = +$ for $H_0 > H_c$. The values of H_0 are set to be $H_0 = 0.386$ (dotted line), 0.4 (dashed line), and 0.5 (solid line), where all the initial conditions are chosen as $s_0 = s_-$.

$= -1/\sqrt{3}$ for H_0 slightly above H_c. The small region including the position $s = -1/\sqrt{3}$ is called the channel. From the symmetry of the system, there also exists the channel near $s = 1/\sqrt{3}$ for $F(t) = -H_0$, as shown in Fig. 1(b). Let us express the positions s_{ch} of the channels as

$$s_{ch} = \begin{cases} -1/\sqrt{3} & \text{if } F(t) = +H_0, \\ +1/\sqrt{3} & \text{if } F(t) = -H_0. \end{cases} \tag{16}$$

The characteristic time τ_{ch} is then defined as the time span that the state point $s(t)$ passes through one of the channels for a constant $F(t)$, either $+H_0$ or $-H_0$. τ_{ch} can be estimated by integrating Eq. (14) around $s \simeq s_{ch}$ as follows. First, consider the case $F(t) = -H_0$. By setting $u(t) = s(t) - s_{ch}$ and assuming $|u| \ll s_{ch}$, Eq. (14) is approximated as

$$\dot{u} = -3s_{ch}u^2 - (H_0 - H_c). \tag{17}$$

This can be integrated to give

$$u(t) = -\sqrt{\frac{H_0 - H_c}{3s_{ch}}} \tan\left[\sqrt{3s_{ch}(H_0 - H_c)} \, t \right] \tag{18}$$

with the initial condition $u(0) = 0$. τ_{ch} is estimated by the condition $u(\tau_{ch}) = \infty$ and thus

$$\tau_{ch} = \frac{C}{(H_0 - H_c)^{1/2}}, \quad C = \frac{\pi}{2\sqrt{3s_{ch}}}. \tag{19}$$

Let us next consider the process that the state point $s(t)$ passes through the channels under DMN. Figure 7 shows temporal evolutions of $s(t)$ numerically obtained for $H_0 = 0.388$ and 0.385. One finds that the time of passing through channels increases as H_0 approaches H_c. The MFPT $\bar{\tau}$ through channels was calculated in Refs. [14,15] by analyzing the master equation. In the present section, we will de-
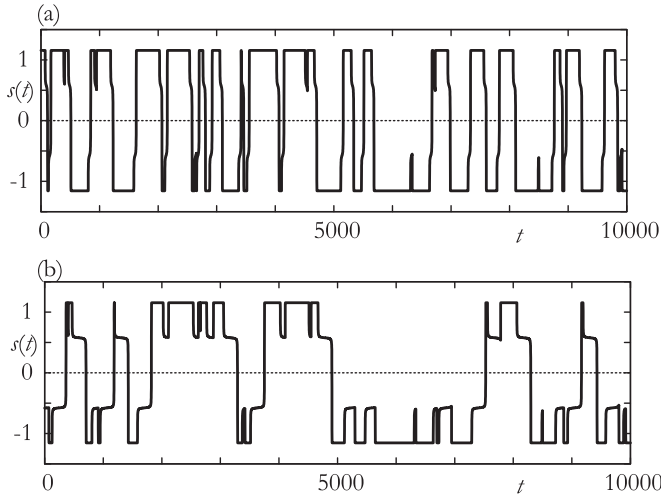
FIG. 7. Time series of $s(t)$ for (a) $H_0 = 0.388$ and (b) 0.385 by keeping $\tau_f = 200$.

rive MFPT in terms of the time scales τ_f and τ_{ch} from a phenomenological viewpoint without use of the analysis made in Refs. [14,15].

The condition for passing through a channel is that $F(t)$ continues to take the identical value either $+H_0$ or $-H_0$ for time longer than τ_{ch}. For H_0 satisfying $\tau_f > \tau_{ch}$, we obtain $p(\tau_{ch}) = e^{-\tau_{ch}/\tau_f} \simeq 1$, which implies that $F(t)$ almost always satisfies the condition for passing through the channel. Therefore, $\bar{\tau}$ in the case of $\tau_f > \tau_{ch}$ is nearly equivalent to τ_{ch}, i.e.,

$$\bar{\tau} \simeq \frac{C}{(H_0 - H_c)^{1/2}}. \qquad (20)$$

In the case of $\tau_f \ll \tau_{ch}$, on the other hand, Eq. (4) gives $p(\tau_{ch}) \ll 1$. This fact implies that the probability that $F(t)$ continues to take the identical value for time longer than τ_{ch} is quite small and hence that $\bar{\tau}$ is much longer than τ_{ch} because it needs a long time to satisfy the condition for the state point to pass through the channel. $\bar{\tau}$ in the case of $\tau_f \ll \tau_{ch}$ is explicitly determined as follows. For a long $\bar{\tau}$, let us divide $\bar{\tau}$ into subintervals each of which has the time span τ_f. The divided individual time series are approximately independent of each other. Therefore, $\tau_f/\bar{\tau}$ is the probability that the state point passes through a channel once because $\bar{\tau}$ is MFPT through the channel. On the other hand, $p(\tau_{ch})$ is identical to the probability for $s(t)$ to pass through the channel once by definition of the probability. Therefore we get the relation $p(\tau_{ch}) \simeq \tau_f/\bar{\tau}$, which leads to

$$\bar{\tau}^{-1} \simeq \tau_f^{-1} e^{-\tau_{ch}/\tau_f} = \tau_f^{-1} \exp\left(-\frac{C}{\tau_f(H_0 - H_c)^{1/2}}\right) \qquad (21)$$

with the constant C defined in Eq. (19). This expression agrees with the result obtained in Refs. [14,15]. Equation (21) reveals that MFPT through the channel depends on $H_0 - H_c$ in a stretched exponential form for $\tau_f \ll \tau_{ch}$, and is quite different from the asymptotic form (20). The above dependence of $\bar{\tau}$ on $H_0 - H_c$ is confirmed in Fig. 8.
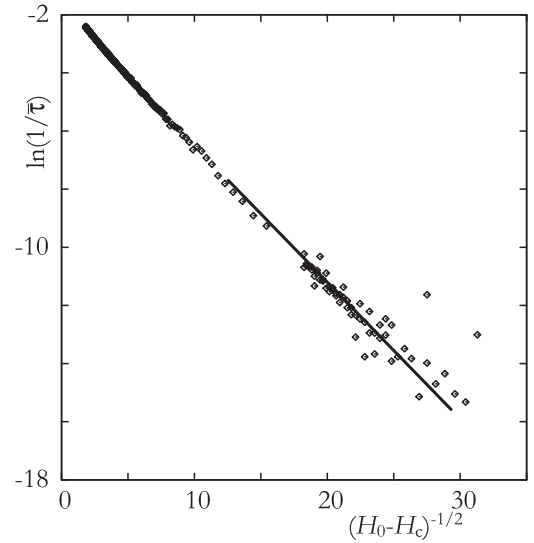

FIG. 8. The dependence of $\bar{\tau}$ on $H_0 - H_c$ determined numerically for $\tau_f = 5$. $\bar{\tau}$ for a given H_0 is obtained by integrating Eq. (3) until a time T and simultaneously by counting the number N of times passing through the position $s = 0$. Then $\bar{\tau}$ is evaluated as $\bar{\tau} = T/N$. One finds that $\ln \bar{\tau}^{-1}$ linearly depends on $(H_0 - H_c)^{-1/2}$ in the region of $0 < H_0 - H_c \ll 1$, where the solid line is expressed as $\ln y = Ax + B$ with fitting coefficients A and B.

IV. PHENOMENOLOGICAL ANALYSIS

In order to discuss statistical characteristics of the dynamics passing through the channels for $\tau_f \ll \tau_{ch}$, we here develop a phenomenological approach. The behaviors of $s(t)$ for which we attempt to model are first summarized. The initial condition of $s(t)$ is set to be in the vicinity of s_+. If a time interval of $F(t)$ satisfying the condition $F(t) = -H_0$ becomes longer than τ_{ch} for the first time, then $s(t)$ passes through s_{ch} and approaches s_- in the time interval. See Fig. 9. The event in which $s(t)$ jumps from s_+ to s_- occurs only in this case. It should be noted that the jumps from $s(t) > 0$ $[s(t) < 0]$ to $s(t) < 0$ $[s(t) > 0]$ are approximately independent of subsequent jumps.

Let us discretize the time t in the form $t = k\Delta t$, ($k = 1, 2, 3, \ldots$) as a simple approach to develop the phenomenological analysis according to the process noted above, where Δt is a certain small time step. Then, τ_{ch} is discretized
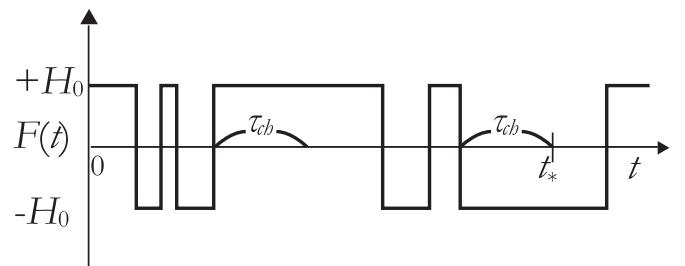

FIG. 9. Time series of $F(t)$ schematically indicating the time that $s(t)$ jumps from s_+ to s_-. $s(t)$ jumps at the time t_* in this case, where $F(t)$ takes the value $-H_0$ longer than τ_{ch} for the first time in the time series of $F(t)$.

as $\tau_{\text{ch}} \equiv n_{\text{ch}}\Delta t$ with the corresponding integer n_{ch}. $F(t)$ is assumed to keep the same value for the interval Δt, which is denoted as $F_k = F(k\Delta t)$. The conditional probability p that F_{j+1} takes the same value as F_j is given by

$$p = e^{-\Delta t/\tau_f}, \qquad (22)$$

and the probability q that F_{k+1} is different from F_k is therefore given by

$$q = 1 - p. \qquad (23)$$

The system is analyzed phenomenologically as follows:

(i) We introduce the variable s_k at a discretized time $k\Delta t$ which takes two values ± 1.

(ii) s_k and F_k are initially set to $s_0 = +1$ and $F_0 = +H_0$, respectively.

(iii) s_k jumps from $+1$ (-1) to -1 $(+1)$ only if F_k continues to take the identical value $-H_0$ $(+H_0)$ for a time interval longer than $n_{\text{ch}}\Delta t$.

(iv) s_k does not jump from $+1$ (-1) to -1 $(+1)$ even though F_k continues to take $+H_0$ $(-H_0)$ for any time interval longer than $n_{\text{ch}}\Delta t$.

A. MFPT $\bar{\tau}$ through the channel

We first derive the exact expression for the MFPT $\bar{\tau}$ through the channel with the phenomenological approach. In considering the time series having F_k, $\bar{\tau}$ is evaluated as

$$\bar{\tau} = \sum_l l\Delta t \sum_{0 \leq k \leq l} g_{k,l}^{(n_{\text{ch}})} q^k p^{l-k} \Big|_{q=1-p}. \qquad (24)$$

Here $g_{k,l}^{(n_{\text{ch}})}$ is the number of the time sequences $\{F_j\}$ for $0 \leq j < l$ satisfying that F_j changed its value k times in each $\{F_j\}$ and s_j jumps from $+1$ to -1 for the first time at $t = l\Delta t$.

Equation (24) is, furthermore, rewritten as

$$\bar{\tau} = \hat{T} Q_{n_{\text{ch}}}(q,p)\big|_{q=1-p} \qquad (25)$$

with the differential operator $\hat{T}$ and the quantity $Q_{n_{\text{ch}}}(q,p)$ defined by

$$\hat{T} \equiv \Delta t \left(q\frac{\partial}{\partial q} + p\frac{\partial}{\partial p} \right) \qquad (26)$$

and

$$Q_{n_{\text{ch}}}(q,p) \equiv \sum_l \sum_{0 \leq k \leq l} g_{k,l}^{(n_{\text{ch}})} q^k p^{l-k}. \qquad (27)$$

One should note that the q and p dependences in $Q_{n_{\text{ch}}}$ are crucial and that q and p are considered to be independent in Eq. (27).

The explicit form of $Q_{n_{\text{ch}}}(q,p)$ is then determined so as to satisfy the following conditions:

(i) In considering any length of time series giving F_k, there exists a time interval of length n_{ch} in the last of the time series, where all the F_k take the same value $-H_0$, i.e., the condition that s_k jumps from $+1$ to -1 is satisfied.

(ii) The condition for s_k to jump from $+1$ to -1 is not satisfied before the last time interval.

One should note that the equality $Q_n(1-p,p) = 1$ holds for any n, because the time interval described above always exists somewhere in a long time series. Particularly, for $n = n_{\text{ch}}$, $Q_{n_{\text{ch}}}(1-p,p)$ is obviously equal to the probability that s_j changes its sign, which must be unity for $H_0 > H_c$.

As shown in Appendix A, the explicit form of $Q_n(q,p)$ is given by

$$Q_n(q,p) = \frac{(1-p)qp^{n-1}}{(1-p)^2 - q^2(1-p^{n-1})}, \qquad (28)$$

where the condition $Q_n(1-p,p) = 1$ is easily confined. Applying the operator (26) to the explicit form (28) with $n = n_{\text{ch}}$ yields the relation

$$\bar{\tau} = \hat{T} Q_{n_{\text{ch}}}(q,p)\big|_{q=1-p} = \Delta t \frac{2 - p^{n_{\text{ch}}-1}}{(1-p)p^{n_{\text{ch}}-1}}$$

$$= \Delta t \frac{2 - e^{\Delta t/\tau_f}e^{-\tau_{\text{ch}}/\tau_f}}{(1 - e^{-\Delta t/\tau_f})e^{\Delta t/\tau_f}e^{-\tau_{\text{ch}}/\tau_f}}, \qquad (29)$$

where the last equality is obtained by using Eqs. (22) and (23) with the relation $\tau_{\text{ch}} = n_{\text{ch}}\Delta t$. The exact expression of $\bar{\tau}$ is finally given by

$$\bar{\tau} = \tau_f(2e^{\tau_{\text{ch}}/\tau_f} - 1) \qquad (30)$$

in the limit of $\Delta t \to 0$ by keeping τ_{ch} constant. Equation (30) qualitatively agrees for $\tau_{\text{ch}}/\tau_f \gg 1$ with the result (21).

B. Distribution function $P(\tau)$ for the passage time τ

The distribution function $P(\tau)$ for the passage time τ through the channel s_{ch} is determined by solving the equation

$$P(\tau) = \delta(\tau - \hat{T}) Q_{n_{\text{ch}}}(q,p)\big|_{q=1-p}, \qquad (31)$$

where $\delta(x)$ is the delta function. The Laplace transform $\mathcal{L}[P](z)$ should be calculated in order to solve Eq. (31). By using the series expansion of $Q_{n_{\text{ch}}}(q,p)$ given by Eq. (27), the Laplace transform of $P(\tau)$ is obtained as

$$\mathcal{L}[P](z) \equiv \int_0^\infty e^{-\tau z} P(\tau) d\tau = e^{-z\hat{T}} Q_{n_{\text{ch}}}(q,p)\big|_{q=1-p}$$

$$= \sum_l \sum_{0 \leq k \leq l} g_{k,l}^{(n_{\text{ch}})}(e^{-z\Delta t}q)^k (e^{-z\Delta t}p)^{l-k} \Big|_{q=1-p}. \qquad (32)$$

Equation (32) implies that $\mathcal{L}[P](z)$ can be obtained by replacing q and p by $e^{-z\Delta t}q$ and $e^{-z\Delta t}p$ in $Q_{n_{\text{ch}}}(q,p)$, respectively, i.e.,

$$\mathcal{L}[P(\tau)](z) = Q_{n_{\text{ch}}}(e^{-z\Delta t}q, e^{-z\Delta t}p)\big|_{q=1-p}. \qquad (33)$$

Substituting the explicit form (28) for $n = n_{\text{ch}}$ into Eq. (33) yields the equation

$$\mathcal{L}[P(\tau)](z) = \frac{(\tau_f z + 1)e^{-(z+\tau_f^{-1})\tau_{\text{ch}}}}{\tau_f^2 z^2 + 2\tau_f z + e^{-(z+\tau_f^{-1})\tau_{\text{ch}}}} \qquad (34)$$

in the limit of $\Delta t \to 0$ by keeping τ_{ch} constant. By applying the inverse Laplace transform to Eq. (34), the distribution

function $P(\tau)$ is analytically evaluated in the series expansion as

$$
\begin{aligned}
P(\tau) &= \tau_f^{-1} e^{-\tau/\tau_f} \sum_{k=0}^{\infty} \theta(t_{k+1}) \left. \frac{(-x)^k}{k!} \frac{d^k}{dx^k} \cosh\sqrt{x} \right|_{x=(t_{k+1})^2} \\
&= \tau_f^{-1} e^{-\tau/\tau_f} \bigg(\theta(t_1)\cosh(t_1) - \theta(t_2)\frac{t_2 \sinh(t_2)}{2} \\
&\quad + \theta(t_3)\frac{t_3^2 \cosh(t_3) - t_3 \sinh(t_3)}{8} \\
&\quad - \theta(t_4)\frac{t_4^3 \sinh(t_4) - 3t_4^2 \cosh(t_4) + 3t_4 \sinh(t_4)}{48} + \cdots \bigg),
\end{aligned}
$$
(35)

where $t_k(\tau) \equiv (\tau - k\tau_{\text{ch}})/\tau_f$ and $\theta(t)$ is the Heaviside function defined by

$$
\theta(t) = \begin{cases} 1 & \text{for } t \geq 0, \\ 0 & \text{for } t < 0. \end{cases}
$$
(36)

For details of the derivation of Eq. (35), see Appendix B.

Let us suppose to truncate the expansion (35) at $k=k_c$ for an arbitrary k_c. It should be noted that Eq. (35) gives the exact distribution for $0 < \tau < k_c\tau_{\text{ch}}$ even though the truncation is executed, since all the terms individually include $\theta(t_k)$ and so the terms for $k > k_c$ do not contribute to $P(\tau)$ for $\tau < k_c\tau_{\text{ch}}$. The analytical result (35) is compared with the numerically evaluated distribution in Fig. 10. One observes that the phenomenological analysis quantitatively explains the statistical property of passing through the channels. The characteristics obtained from the figure are summarized as follows.

(i) There exists a region where $P(\tau)=0$ for $\tau < \tau_{\text{ch}}$, which presents the minimal time of passing through the channels.

(ii) $P(\tau)$ decreases exponentially for $\tau \gg \tau_{\text{ch}}$, $P(\tau) \propto e^{-\alpha\tau}$ with a constant α.

(iii) The rate α increases as τ_f is increased. This tendency is consistent with the fact that the probability of passing through channels increases as τ_f is increased since DMN will often continue to take an identical value longer than τ_{ch}.

On the other hand, the expansion (35) disagrees with the correct value in an exponential way for $\tau > k_c\tau_{\text{ch}}$. Let us try to obtain the asymptotic solution of $P(\tau)$ for $\tau \gg \tau_{\text{ch}}$. Equation (B2) is approximated as

$$
\langle e^{-z(\tau-\tau_{\text{ch}})} \rangle \simeq \frac{1}{1 + (\bar{\tau} - \tau_{\text{ch}})z} \quad \text{for } |z| \ll \tau_{\text{ch}}^{-1},
$$
(37)

where $\bar{\tau}$ is MFPT given in Eq. (30). The inverse Laplace transform of Eq. (37) is straightforwardly calculated to give

$$
P(\tau) \simeq \frac{1}{\bar{\tau} - \tau_{\text{ch}}} \exp\left(-\frac{\tau - \tau_{\text{ch}}}{\bar{\tau} - \tau_{\text{ch}}} \right),
$$
(38)

which reveals that $P(\tau)$ decreases exponentially with the damping rate $\alpha = (\bar{\tau} - \tau_{\text{ch}})^{-1}$ for $\tau \gg \tau_{\text{ch}}$.
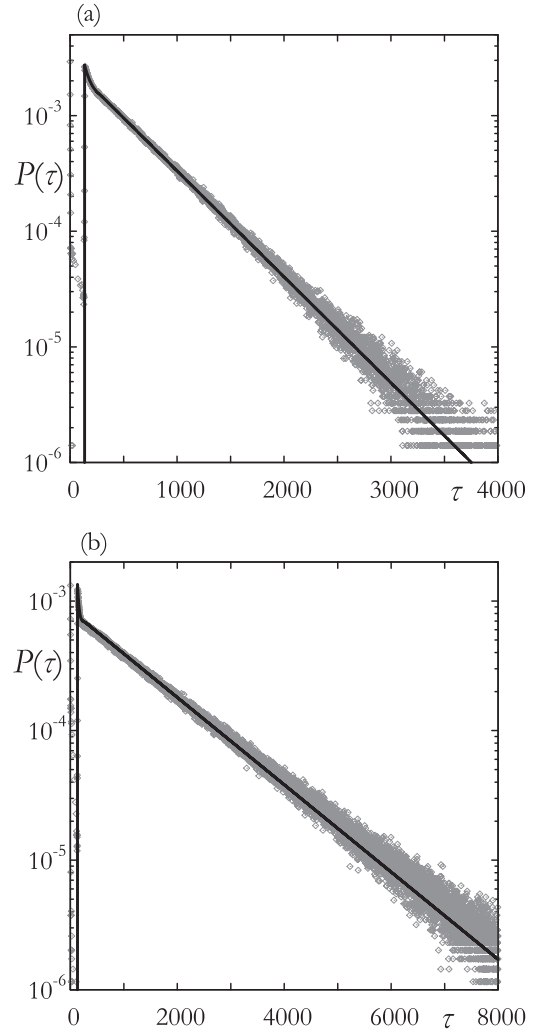

FIG. 10. Distribution function $P(\tau)$ of time passing through channels. The theoretical results (solid lines) are compared with the numerically evaluated distributions (symbols) for (a) $\tau_f=130$ and (b) $\tau_f=50$. The strength of DMN is set to be $H_0=0.3852$ in both of the numerical simulations. τ_{ch} corresponding to the applied DMN is estimated to be $\tau_{\text{ch}} \simeq 134$ via the condition $P(\tau) \simeq 0$ for $\tau < \tau_{\text{ch}}$, where both (a) and (b) give the identical value of τ_{ch}. The expansion in Eq. (35) is summed over for $k \leq 60$, i.e., $k_c=60$.

C. Fourier spectrum determined by the phenomenological analysis

We derive the Fourier spectrum of a time series $s(t)$ by the phenomenological analysis to focus on the dynamical characteristics in the SRM phase. The Fourier spectrum $I_x(\omega)$ is defined by

$$
I_x(\omega) = \lim_{T\to\infty} \frac{1}{T} \left\langle \left| \int_0^T x(t)e^{-i\omega t}dt \right|^2 \right\rangle,
$$
(39)

i.e., the ensemble average of the Fourier transform of a time series $x(t)$.

Let us first consider $s_0(t) \equiv \text{sgn}[s(t)]$. Then the time series $s_0(t)$ is expressed as

$$s_0(t) = (-1)^{n-1} \quad \text{for } t_{n-1} \leqslant t < t_n \qquad (40)$$

with $n \geqslant 1$, where t_n denotes the nth time to cross zero for $s(t)$. Hereafter, t_0 is set to be zero without loss of generality. By identifying that $\tau_n \equiv t_n - t_{n-1}$ is independently distributed according to Eq. (35), one obtains the Fourier spectrum of $s_0(t)$ by the phenomenological analysis shown in Appendix C, in the form

$$I_{s_0}(\omega) = \frac{4}{\bar{\tau}\omega^2} \operatorname{Re}\left(\frac{1 - \langle e^{-i\omega\tau_n}\rangle}{1 + \langle e^{-i\omega\tau_n}\rangle}\right) = \frac{4}{\bar{\tau}\omega^2} \frac{1 - |\langle e^{-i\omega\tau_n}\rangle|^2}{|1 + \langle e^{-i\omega\tau_n}\rangle|^2}, \qquad (41)$$

where $\operatorname{Re}(X)$ represents the real part of X, and $\lim_{N\to\infty} \frac{t_N}{N} = \langle \tau_n \rangle = \bar{\tau}$ is used.

Substituting the explicit form of $\langle e^{-i\omega\tau_n}\rangle$ given in Eq. (34) with $z = i\omega$ into Eq. (41) yields

$$I_{s_0}(\omega) = \left(\frac{4\tau_f}{\bar{\tau}\omega}\right)\frac{\omega^3\tau_f^3 + (4 - e^{-2\tau_{\text{ch}}/\tau_f})\omega\tau_f - 2e^{-\tau_{\text{ch}}/\tau_f}(\omega\tau_f\cos\omega\tau_{\text{ch}} + 2\sin\omega\tau_{\text{ch}})}{(4 + \omega^2\tau_f^2)(\omega^2\tau_f^2 - 2\omega\tau_f e^{-\tau_{\text{ch}}/\tau_f}\sin\omega\tau_{\text{ch}} + e^{-2\tau_{\text{ch}}/\tau_f})}. \qquad (42)$$

The above result is confirmed by comparing with the numerically evaluated Fourier spectrum for the normalized time series $s_0(t)$ in Fig. 11.

Let us finally modify the phenomenological analysis which is compatible with the numerically evaluated spectrum of the original time series $s(t)$ without normalization. Instead of Eq. (40), let us define

$$\tilde{s}(t) = (-1)^{n-1}[1 - a(t - t_{n-1})] \quad \text{for } t_{n-1} \leqslant t < t_n \quad (43)$$

with $n \geqslant 1$, where $a(\Delta t)$ incorporates the wave form of the time series passing through the channel and is assumed to be $a(\Delta t) = 0$ for $\Delta t > \tau_{\text{ch}}$. Note that by setting $a(\Delta t) = 0$ also for $\Delta t \leqslant \tau_{\text{ch}}$ the result of original phenomenological analysis is recovered. As shown in Appendix C, the Fourier spectrum $I_{\tilde{s}}(\omega)$ for $\tilde{s}(t)$ as a modification to $I_{s_0}(\omega)$ is obtained in the form

$$I_{\tilde{s}}(\omega) = I_{s_0}(\omega)\frac{1 + |\hat{a}(\omega)|^2 + 2\operatorname{Re}[\hat{a}(\omega)]}{4}, \qquad (44)$$

where

$$\hat{a}(\omega) \equiv 1 - i\omega\int_0^{\tau_{\text{ch}}} a(t)e^{-i\omega t}dt. \qquad (45)$$

By approximating as $a(\Delta t) = 1 + |s_{\text{ch}}|$ for $0 < \Delta t < \tau_{\text{ch}}$, Eq. (44) reduces to

$$I_{\tilde{s}}(\omega) = I_{s_0}(\omega)\left(\frac{1 + s_{\text{ch}}^2}{2} + \frac{1 - s_{\text{ch}}^2}{2}\cos\omega\tau_{\text{ch}}\right). \qquad (46)$$

Equation (46) is confirmed by comparing with the numerically evaluated Fourier spectrum in Fig. 12.
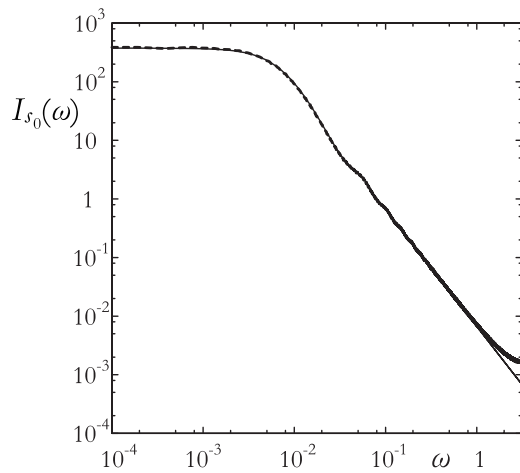

FIG. 11. Fourier spectrum of $s_0(t)$ obtained theoretically (solid line) and numerically (dashed line). $\tau_f = 130$ is set for both numerical and theoretical results, and the strength of DMN is set to be $H_0 = 0.3852$ in the numerical simulation. $\tau_{\text{ch}} = 134$ estimated in Fig. 10 is used for Eq. (42).
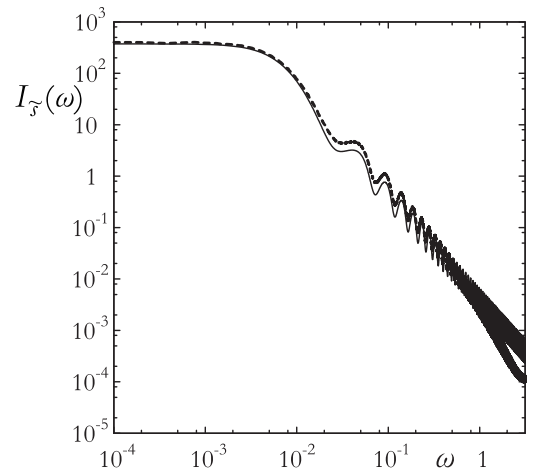

FIG. 12. Theoretically obtained Fourier spectrum (46) (solid line) with $|s_{\text{ch}}| = 1/\sqrt{3}$ is compared with the numerical result (dashed line). $\tau_f = 130$ is set for both numerical and theoretical results, and the strength of DMN is set to be $H_0 = 0.3852$ in the numerical simulation. $\tau_{\text{ch}} = 134$ is used for Eq. (42) which was estimated in Fig. 10.

V. CONCLUDING REMARKS

In this paper, we used the model equation (3) under the dichotomous Markov noise (DMN) $F(t)$ with a finite correlation time in order to investigate the dynamics of the magnetization $s(t)$ of the ferromagnet system driven by the magnetic field applied in one direction, where its strength is constant and only the direction temporally changes. It was found that the dynamics of $s(t)$ show two kinds of motion, i.e., the symmetry-restoring motion (SRM) and the symmetry-breaking motion (SBM), which are, respectively, observed when H_0 is above and below the critical value H_c. The transition line between SRM and SBM was determined only by the strength of the applied DMN and is independent of the correlation time τ_f of DMN. By observing the distribution functions of $s(t)$ for SRM and SBM, the ensemble average of $s(t)$ discontinuously changes at $H_0=H_c$. These results are quite different from those in the system driven by a periodically oscillating field [7].

We then discussed the mean first passage time (MFPT) slightly above H_c and found that it depends on H_0-H_c and τ_f as

$$\bar{\tau} \simeq \tau_f \exp\left(\frac{C}{\tau_f(H_0-H_c)^{1/2}}\right). \tag{47}$$

This anomalous characteristics has a form similar to that of the average duration between neighboring phase slips of the phase difference in the phase synchronization observed in coupled chaotic systems [20]. Furthermore, a phenomenological approach was proposed to analytically discuss the statistical characteristics for $H_0>H_c$. By obtaining the probability $Q_n(q,p)$ of $s(t)$ passing through the channel, the MFPT $\bar{\tau}$, the distribution function $P(\tau)$ of the passage time τ and the Fourier spectrum $I(\omega)$ of the time series were obtained by using the phenomenological analysis. The statistics obtained by the phenomenological analysis were found to be not only in qualitative but also in quantitative agreement with the numerically obtained results.

In closing the paper, it is worth noting that the effect of DMN on nonlinear dynamical systems is generally quite different from that of Gaussian noise and DMN produces a new dynamical response of the systems. It is highly desired to examine the statistical characteristics obtained in this paper in laboratory experiments, and also in other numerical simulations, e.g., Monte Carlo simulations.

APPENDIX A: EXPLICIT FORM OF $Q_n(q,p)$

First of all, notice that each sample path of F_k ($k=0,1,2,\ldots$) corresponds to a symbol sequence of $\{+, -\}$.

Let w be a symbol sequence of $\{+, -\}$, which is referred to as a string. For given sets A and B of strings, let AB be the set of all strings expressed as ab for $a \in A$ and $b \in B$, where ab denotes the concatenated string of a followed by b. In the following, the set composed of only one string w will be simply expressed as w. Furthermore, let $(A)_n$ be the set of all strings expressed as

$$a_1 a_2 \cdots a_k \tag{A1}$$

with $a_i \in A$ and $0 \leqslant k \leqslant n$, where $k=0$ means the zero length string, including the case $a_i=a_j$ for $i \neq j$. Then, with this notation, every possible sequence starting with plus signs and terminating with successive minus signs of length n ($n \geqslant 2$), which first appears in that string, can be expressed as

$$S_n \equiv \left(+ (+)_\infty - (-)_{n-2}\right)_\infty + (+)_\infty \overbrace{-- \cdots -}^{n\ \text{symbols}}. \tag{A2}$$

For a given set S of strings, let us define its "probability" as a function of p and q by

$$P(q,p;S) \equiv \sum_{w \in S} P_w(p,q), \tag{A3}$$

where $P_w(p,q) \equiv p^{k(w)} q^{l(w)}$ denotes the probability for a string w, and $k(w)$ and $l(w)$ denote the numbers of pairs of identical symbols ($--$, $++$) and different symbols ($-+$, $+-$) appearing in w, respectively. For given strings w_1 and w_2, obviously, the identity

$$P_{w_1 w_2}(q,p) = P_{w_1 \sigma}(q,p) P_{w_2}(q,p) \tag{A4}$$

holds with σ being the first symbol in w_2, and we call $w_1\sigma$ and w_2 a decomposition of the string $w \equiv w_1 w_2$. By noting that

$$Q_n(q,p) = P(q,p;S_n) \tag{A5}$$

and considering decompositions of each element in S_n, $Q_n(q,p)$ can be expressed as

$$Q_n(q,p) = P(q,p;S'_n) P(q,p;R) p^{n-1}, \tag{A6}$$

where

$$S'_n \equiv \left(+ (+)_\infty - (-)_{n-2}\right)_\infty + \tag{A7}$$

and

$$R \equiv + (+)_\infty -. \tag{A8}$$

Since each element of S'_n can be uniquely decomposed into a multiple of elements in

$$S''_n \equiv + (+)_\infty - (-)_{n-2} + \tag{A9}$$

and inversely every multiple of elements in S''_n uniquely corresponds to an element in S'_n as its decomposition, we obtain

$$P(q,p;S'_n) = \sum_{j=0}^{\infty} [P(q,p;S''_n)]^j \tag{A10}$$

$$= \frac{1}{1 - P(q,p;S_n'')}. \tag{A11}$$

Finally, $P(q,p;R)$ and $P(q,p;S_n'')$ are calculated as

$$P(q,p;R) = q\sum_{j=0}^{\infty} p^j = \frac{q}{1-p} \tag{A12}$$

and

$$P(q,p;S_n'') = \sum_{j=0}^{\infty} p^j q \sum_{i=0}^{n-2} p^i q = q^2 \frac{1-p^{n-1}}{(1-p)^2}, \tag{A13}$$

which yield Eq. (28) together with (A6) and (A11).

APPENDIX B: DERIVATION OF THE PROBABILITY DISTRIBUTION FUNCTION $P(\tau)$

Let us evaluate the inverse Laplace transform of Eq. (34) in order to derive the explicit form of $P(\tau)$. For simplicity, the time is rescaled as $\tau_f = 1$. Then Eq. (34) is rewritten as

$$\langle e^{-z\tau} \rangle = \frac{(1+z)e^{-(1+z)\tau_{\text{ch}}}}{(1+z)^2 - [1 - e^{-(1+z)\tau_{\text{ch}}}]}, \tag{B1}$$

which reads

$$\mathcal{L}[P(\tau + \tau_{\text{ch}})] = \langle e^{-z(\tau - \tau_{\text{ch}})} \rangle = \frac{e^{-\tau_{\text{ch}}}}{1 + z - \dfrac{1 - e^{-(1+z)\tau_{\text{ch}}}}{1+z}}$$

$$= e^{-\tau_{\text{ch}}}\sum_{n=0}^{\infty} \frac{(1 - e^{-(1+z)\tau_{\text{ch}}})^n}{(1+z)^{2n+1}}. \tag{B2}$$

Repeatedly applying the formula

$$\mathcal{L}^{-1}[e^{-(1+z)\tau_{\text{ch}}}\hat{f}(z)] = e^{-\tau_{\text{ch}}}f(\tau - \tau_{\text{ch}})$$

$$= e^{-\tau_{\text{ch}}}e^{-\tau_{\text{ch}}(d/d\tau)}f(\tau)$$

$$= e^{-\tau_{\text{ch}}}e^{-\tau_{\text{ch}}(d/d\tau)}\mathcal{L}^{-1}[\hat{f}(z)] \tag{B3}$$

with $f(\tau) \equiv \mathcal{L}^{-1}[\hat{f}(z)]$, one obtains

$$\mathcal{L}^{-1}\left(\frac{(1 - e^{-(1+z)\tau_{\text{ch}}})^n}{(1+z)^{2n+1}}\right) = (1 - e^{-\tau_{\text{ch}}}e^{-\tau_{\text{ch}}(d/d\tau)})^n \mathcal{L}^{-1}\left(\frac{1}{(1+z)^{2n+1}}\right)$$

$$= (1 - e^{-\tau_{\text{ch}}}e^{-\tau_{\text{ch}}(d/d\tau)})^n \frac{\tau^{2n}}{(2n)!}e^{-\tau}\theta(\tau), \tag{B4}$$

where $\theta(\tau)$ denotes the Heaviside function Eq. (36), and the formula

$$\mathcal{L}^{-1}\left(\frac{1}{(1+z)^m}\right) = \frac{\tau^{m-1}}{(m-1)!}e^{-\tau}\theta(\tau) \tag{B5}$$

for any positive integer m was used. Thus, the inverse Laplace transform of Eq. (B2) reads

$$P(\tau + \tau_{\text{ch}}) = e^{-\tau_{\text{ch}}}\sum_{n=0}^{\infty} (1 - e^{-\tau_{\text{ch}}}e^{-\tau_{\text{ch}}(d/d\tau)})^n \frac{\tau^{2n}}{(2n)!}e^{-\tau}\theta(\tau)$$

$$= e^{-(\tau + \tau_{\text{ch}})}\sum_{n=0}^{\infty} (1 - e^{-\tau_{\text{ch}}(d/d\tau)})^n \frac{\tau^{2n}}{(2n)!}\theta(\tau), \tag{B6}$$

where the identity

$$e^{-\tau_{\text{ch}}}e^{-\tau_{\text{ch}}(d/d\tau)}e^{-\tau} = e^{-\tau}e^{-\tau_{\text{ch}}(d/d\tau)} \tag{B7}$$

was applied. By noting the identity

$$(1 - e^{-\tau_{\text{ch}}(d/d\tau)})^n = \sum_{k=0}^{n} \frac{(-e^{-\tau_{\text{ch}}(d/d\tau)})^k}{k!}\left.\frac{d^k x^n}{dx^k}\right|_{x=1}$$

$$= \sum_{k=0}^{\infty} \frac{e^{-k\tau_{\text{ch}}(d/d\tau)}(-1)^k}{k!}\left(\frac{d}{dx}\right)^k x^n \bigg|_{x=1}, \tag{B8}$$

Eq. (B6) is further simplified as

$$P(\tau + \tau_{\text{ch}}) = e^{-(\tau + \tau_{\text{ch}})}\sum_{n=0}^{\infty}\sum_{k=0}^{\infty} e^{-k\tau_{\text{ch}}(d/d\tau)}\frac{(-1)^k}{k!}\left(\frac{d}{dx}\right)^k x^n \frac{\tau^{2n}}{(2n)!}\theta(\tau)\bigg|_{x=1} = e^{-(\tau + \tau_{\text{ch}})}\sum_{k=0}^{\infty} e^{-k\tau_{\text{ch}}(d/d\tau)}\frac{(-1)^k}{k!}\left(\frac{d}{dx}\right)^k \cosh(\sqrt{x}\tau)\theta(\tau)\bigg|_{x=1}$$

$$= e^{-(\tau + \tau_{\text{ch}})}\sum_{k=0}^{\infty} e^{-k\tau_{\text{ch}}(d/d\tau)}\theta(\tau)\frac{(-\tau^2)^k}{k!}\left(\frac{d}{dx}\right)^k \cosh\sqrt{x}\bigg|_{x=\tau^2} = e^{-(\tau + \tau_{\text{ch}})}\sum_{k=0}^{\infty} \theta(t_k)\frac{(-x)^k}{k!}\frac{d^k}{dx^k}\cosh\sqrt{x}\bigg|_{x=t_k^2}, \tag{B9}$$

where $t_k(\tau) \equiv \tau - k\tau_{\text{ch}}$ and the formula $\sum_{n=0}^{\infty}\frac{x^n}{(2n)!} = \cosh\sqrt{x}$ was used. After the replacement $\tau \to \tau - \tau_{\text{ch}}$ and the rescaling of time as $\tau \to \tau/\tau_f$ and $\tau_{\text{ch}} \to \tau_{\text{ch}}/\tau_f$, Eq. (B9) reduces to Eq. (35).

APPENDIX C: DERIVATION OF THE FOURIER SPECTRUM $I(\omega)$

In this appendix, we derive the Fourier spectrum of the time series of the magnetization $s(t)$ for the phenomenologi-

cal analysis. Let $\tau_1, \tau_2, \tau_3, \ldots$ be a sequence of mutually independent random variables having the probability density $P(\tau)$ obeying the condition $P(\tau) = 0$ for $\tau < \tau_{ch}$, i.e., $\tau_k \geq \tau_{ch}$. We introduce the variable

$$\tilde{s}(t) = (-1)^n[1 - a(t - t_{n-1})] \quad \text{for } t_{n-1} \leq t < t_n, \quad \text{(C1)}$$

where $t_n \equiv \Sigma_{k=1}^N \tau_k$ and $a(\Delta t)$ is a function satisfying $a(\Delta t) = 0$ for $\Delta t > \tau_{ch}$. We assume that the time series of the magnetization $s(t)$ is approximately expressed by $\tilde{s}(t)$ with an appropriate form of $a(t)$. The Fourier transform of $\tilde{s}(t)$ follows

$$\int_0^{t_N} \tilde{s}(t) e^{-i\omega t} dt = \sum_{n=1}^N (-1)^{n-1} \int_{t_{n-1}}^{t_n} [1 - a(t - t_{n-1})] e^{-i\omega t} dt$$

$$= \sum_{n=1}^N (-1)^{n-1} e^{-i\omega t_{n-1}}$$

$$\times \left(\int_0^{\tau_n} e^{-i\omega t} dt - \int_0^{\tau_{ch}} a(t) e^{-i\omega t} dt \right)$$

$$= \sum_{n=1}^N (-1)^n e^{-i\omega t_{n-1}} \frac{e^{-i\omega \tau_n} - \hat{a}(\omega)}{i\omega}, \quad \text{(C2)}$$

where

$$\hat{a}(\omega) \equiv 1 - i\omega \int_0^{\tau_{ch}} a(t) e^{-i\omega t} dt. \quad \text{(C3)}$$

Considering the absolute square of Eq. (C2) and then taking the ensemble average, we obtain

$$\omega^2 \left| \int_0^{t_N} \tilde{s}(t) e^{-i\omega t} dt \right|^2 = \sum_{n=1}^N |e^{-i\omega \tau_n} - \hat{a}(\omega)|^2$$

$$+ 2 \text{Re}\left(\sum_{1 \leq m < n \leq N} (-1)^{n-m} \right.$$

$$\times e^{-i\omega \Sigma_{k=m+1}^{n-1} \tau_k} [e^{-i\omega \tau_n} - \hat{a}(\omega)]$$

$$\times \left. [1 - e^{-i\omega \tau_m} \hat{a}^*(\omega)] \right) \quad \text{(C4)}$$

and

$$\frac{\omega^2}{N} \left\langle \left| \int_0^{t_N} \tilde{s}(t) e^{-i\omega t} dt \right|^2 \right\rangle$$

$$= 1 + |\hat{a}(\omega)|^2 - 2 \text{Re}[\langle e^{-i\omega \tau_n} \rangle \hat{a}^*(\omega)]$$

$$+ 2N^{-1} \text{Re}\left(\sum_{1 \leq m < n \leq N} (-1)^{n-m} \langle e^{-i\omega \tau_k} \rangle^{n-m-1} \right.$$

$$\times \left. [\langle e^{-i\omega \tau_k} \rangle - \hat{a}(\omega)][1 - \langle e^{-i\omega \tau_k} \rangle \hat{a}^*(\omega)] \right). \quad \text{(C5)}$$

Since $|\langle e^{-i\omega \tau_n} \rangle| < 1$, in the limit of $N \to \infty$, the last term in Eq. (C5) reads

$$-2 \text{Re}\left(\sum_{k=0}^\infty (-1)^k \langle e^{-i\omega \tau_n} \rangle^k [\langle e^{-i\omega \tau_n} \rangle - \hat{a}(\omega)] \right.$$

$$\times \left. [1 - \langle e^{-i\omega \tau_n} \rangle \hat{a}^*(\omega)] \right)$$

$$= -2 \text{Re}\left(\frac{\langle e^{-i\omega \tau_n} \rangle [1 + |\hat{a}(\omega)|^2] - \hat{a}(\omega) - \langle e^{-i\omega \tau_n} \rangle^2 \hat{a}^*(\omega)}{1 + \langle e^{-i\omega \tau_n} \rangle} \right),$$

$$\text{(C6)}$$

which leads to

$$\lim_{N \to \infty} \frac{1}{N} \left\langle \left| \int_0^{t_N} \tilde{s}(t) e^{-i\omega t} dt \right|^2 \right\rangle$$

$$= \omega^{-2} \text{Re}\left(\frac{1 - \langle e^{-i\omega \tau_n} \rangle}{1 + \langle e^{-i\omega \tau_n} \rangle} \right) \{1 + |\hat{a}(\omega)|^2 + 2 \text{Re}[\hat{a}(\omega)]\}.$$

$$\text{(C7)}$$

Noting that $\lim_{N \to \infty} \frac{t_N}{N} = \langle \tau_n \rangle = \bar{\tau}$, we obtain

$$I_{\tilde{s}}(\omega) = I_{s_0}(\omega) \frac{1 + |\hat{a}(\omega)|^2 + 2 \text{Re}[\hat{a}(\omega)]}{4}, \quad \text{(C8)}$$

where

$$I_{s_0}(\omega) \equiv \frac{4}{\omega^2 \bar{\tau}} \text{Re}\left(\frac{1 - \langle e^{-i\omega \tau_n} \rangle}{1 + \langle e^{-i\omega \tau_n} \rangle} \right) \quad \text{(C9)}$$

corresponds to the case that $a(\Delta t) = 0$ for all $\Delta t \geq 0$ and thus $s_0(t) = (-1)^n$ for $t_{n-1} \leq t < t_n$.

[1] T. Tomé and M. J. de Oliveira, Phys. Rev. A **41**, 4251 (1990); J. F. F. Menders and E. J. S. Large, J. Stat. Phys. **64**, 653 (1991).

[2] W. S. Lo and R. A. Pelcovits, Phys. Rev. A **42**, 7471 (1990).

[3] M. Acharyya, Phys. Rev. E **56**, 1234 (1997); **56**, 2407 (1997); **58**, 179 (1998); **59**, 218 (1999).

[4] S. W. Sides, P. A. Rikvold, and M. A. Novotny, Phys. Rev. Lett. **81**, 834 (1998); Phys. Rev. E **59**, 2710 (1999).

[5] P. A. Rikvold *et al.*, in *Computer Simulation Studies in Condensed Matter Physics XIII*, edited by D. P. Landau, S. P. Lewis, and H.-B. Schüttler (Springer, Berlin, 2000), pp. 105–119.

[6] G. Korniss, C. J. White, P. A. Rikvold, and M. A. Novotny, Phys. Rev. E **63**, 016120 (2001).

[7] H. Fujisaka, H. Tutu, and P. A. Rikvold, Phys. Rev. E **63**, 036109 (2001).

[8] H. Tutu and N. Fujiwara, J. Phys. Soc. Jpn. **73**, 2680 (2004).

[9] T. Yasui, H. Tutu, M. Yamamoto, and H. Fujisaka, Phys. Rev. E **66**, 036123 (2002).

[10] Q. Jiang, H.-N. Yang, and G.-C. Wang, Phys. Rev. B **52**, 14911 (1995); J. Appl. Phys. **79**, 5122 (1996).

[11] N. G. Van Kampen, *Stochastic Processes in Physics and Chemistry* (North-Holland, Amsterdam, 1981).

[12] K. Kitahara, W. Horsthemke, and R. Lefever, Phys. Lett. **70A**, 377 (1979); K. Kitahara, W. Horsthemke, R. Lefever, and Y. Inaba, Prog. Theor. Phys. **64**, 1233 (1980).

[13] I. Bena, C. Van den Broeck, R. Kawai, and K. Lindenberg, Phys. Rev. E **66**, 045603(R) (2002); **68**, 041111 (2003).

[14] I. L'Heureux and R. Kapral, J. Chem. Phys. **88**, 7468 (1988); **90**, 2453 (1989); J. M. Porrà, J. Masoliver, and K. Lindenberg, Phys. Rev. A **44**, 4866 (1991); J. M. Porrà, J. Masoliver, K. Lindenberg, I. L'Heureux, and R. Kapral, *ibid.* **45**, 6092 (1992).

[15] P. Hänggi and P. Riseborough, Phys. Rev. A **27**, 3379 (1983); C. Van den Broeck and P. Hänggi, *ibid.* **30**, 2730 (1984); J. M. Sancho, *ibid.* **31**, 3523 (1985); J. Masoliver, K. Lindenberg, and B. J. West, *ibid.* **34**, 2351 (1986); M. A. Rodriguez and L. Pesquera, *ibid.* **34**, 4532 (1986).

[16] W. Horsthemke and R. Lefever, *Noise-Induced Transitions* (Springer, Berlin, 1984), Chap. 9.

[17] I. Bena, e-print cond-mat/0606116.

[18] E. Ott, *Chaos in Dynamical Systems* (University Press, Cambridge, 1993), Sec. 8.3.

[19] There exist several techniques in the case that $F(t)$ is a white noise. See, e.g., C. W. Gardiner, *Handbook of Stochastic Methods* (Springer, Berlin, 1983); H. Risken, *The Fokker-Planck Equation* (Springer, Berlin, 1984).

[20] See, e.g., M. G. Rosenblum, A. S. Pikovsky, and J. Kurths, Phys. Rev. Lett. **76**, 1804 (1996); A. Pikovsky, G. Osipov, M. Rosenblum, M. Zaks, and J. Kurths, *ibid.* **79**, 47 (1997); S. Boccaletti, E. Allaria, R. Meucci, and F. T. Arecchi, *ibid.* **89**, 194101 (2002); E. Rosa, E. Ott, and M. H. Hess, *ibid.* **80**, 1642 (1998); K. J. Lee, Y. Kwak, and T. K. Lim, *ibid.* **81**, 321 (1998); H. Fujisaka, T. Yamada, G. Kinoshita, and T. Kono, Physica D **205**, 41 (2005); H. Fujisaka, S. Uchiyama, and T. Horita, Prog. Theor. Phys. **114**, 289 (2005).